arXiv:1110.1013v2 [math.GT] 13 May 2012

Mapping classes associated to mixed-sign Coxeter graphs

Eriko Hironaka*

May 15, 2012

Abstract

In this paper we investigate mapping classes on oriented surfaces of finite type constructed from Coxeter graphs with extra structure called mixed-sign Coxeter graphs. As in Thurston's construction for classical bipartite Coxeter graphs, properties of the mapping classes reflect properties of the corresponding Coxeter systems. A feature of the more general setting is that, whereas for classical Coxeter graphs the dilatations of pseudo-Anosov examples are bigger than or equal to Lehmer's number, the dilatations of pseudo-Anosov mixed-sign Coxeter mapping classes can be made arbitrarily close to one. We verify that the minimum dilatation orientable mapping classes of genus 2,3,4, and 5 found by Lanneau and Thiffeault can be obtained by this construction. Further, we find a sequence of graphs whose associated mapping classes are pseudo-Anosov, have unbounded genus, and whose genus-normalized dilatations converge to one plus the golden mean, which is the smallest known accumulation point of genus-normalized dilatations.

1 Introduction

In this paper we define and study properties of a family of mapping classes, called *mixed-sign Coxeter mapping classes*, associated to Coxeter graphs Γ with extra structure. As we will show, these mapping classes have the property that if (S, ϕ) is the mapping class associated to a mixed-sign graph $(\Gamma, \mathfrak{s})$, then the spectral radius of the action of ϕ on the homology group $H_1(S; \mathbb{R})$, or the *homological dilatation* $\lambda_{\text{hom}}(\phi)$, equals the spectral radius of the generalized Coxeter element of $(\Gamma, \mathfrak{s})$.

Mapping classes associated to bipartite Coxeter graphs have been studied in [38] [25]. For pseudo-Anosov mapping classes, the minimum dilatation is bounded away from 1 in this family. We will show, however, that Mixed-sign Coxeter pseudo-Anosov mapping classes can have dilatations arbitrarily close to 1.

Given a mapping class (S, ϕ), the *closure* of (S, ϕ) is the pair $(\overline{S}, \overline{\phi})$ where $\overline{S}$ is the closed surface obtained from S by filling in boundary components with disks, and $\overline{\phi}$ is the isotopy class of the extension to $\overline{S}$ of any homeomorphism in the equivalence class of ϕ.

---

*This work was partially supported by a grant from the Simons Foundation (#209171 to Eriko Hironaka).

Question 1.1 *For which g can the minimum dilatation orientable pseudo-Anosov mapping classes on a closed surface of genus g be realized as the closure of a mixed-sign Coxeter mapping class?*

We verify that the minimum dilatation orientable mapping classes for genus 2,3,4, and 5 are realizable as the closures of mixed-sign Coxeter mapping classes.

Our main result, is the following.

Theorem 1.2 *The set of genus-normalized dilatations of closures of orientable pseudo-Anosov mixed-sign Coxeter mapping classes has accumulation point ℓ_0.*

Background. Let S be a compact oriented surface with negative topological Euler characteristic. A *mapping class*, which we usually denote as a pair (S, ϕ), is an isotopy class ϕ of a self-homeomorphism of S that fixes the boundary of S. A mapping class (S, ϕ) is *pseudo-Anosov* if there is a representative f of ϕ, and an associated pair of f- invariant *stable* and *unstable* transverse measured singular foliations $(\mathcal{F}^{\pm}, \nu^{\pm})$ so that $f_* \nu^{\pm} = \lambda_f^{\pm 1} \nu$ for some $\lambda_f > 1$. The expansion factor $\lambda(\phi) = \lambda_f$ is called the *(geometric) dilatation* of (S, ϕ) and is written $\lambda(\phi)$ or $\lambda_{\text{geo}}(\phi)$. A pseudo-Anosov mapping class is *orientable* if its associated stable and unstable foliations are orientable, or equivalently if its homological and geometric dilatations are equal.

Let Γ be a simply-laced Coxeter graph, and let $\mathcal{G} = \{\gamma_1, \dots, \gamma_k\}$ be a finite collection of simple closed curves in general position on a compact oriented surface S, so that the intersection matrix of $\mathcal{G}$ equals the incidence matrix for Γ. The pair $(S, \mathcal{G})$ is called a geometric realization of Γ. The mapping class group of an oriented surface S of finite type can be presented as the image of a homomorphism

$$\rho : \mathcal{A}(\Gamma) \to \text{Mod}(S)$$

of the Artin group $\mathcal{A}(\Gamma)$ of a Coxeter graph Γ with the addition of a finite set of generators [4] [9][22] [23] [20] [26] [27] [41]. Here the generators of $\mathcal{A}(\Gamma)$ map to Dehn twists around simple closed curves The pair $(S, \mathcal{G})$ is called a *geometric realization* of Γ. Pseudo-Anosov mapping classes with computable invariants realized as the product of these generators were studied in [38] [13] [25] [30] under restrictive conditions. The constructions in this paper apply to all simply-laced Coxeter graphs, and we add additional sign labels on vertices.

Let $\mathcal{P}$ be the union of pseudo-Anosov mapping classes defined on compact oriented surfaces of negative Euler characteristic. The minimum dilatation δ_g for pseudo-Anosov mapping classes on closed surfaces of genus g is only known for genus 2 [8]. For orientable classes the minimum dilatation is known for genus 2,3,4,5,7,8 [24] [14] [1] [21]. The *genus-normalized dilatation* of a mapping class (S, ϕ) defined on a closed genus g surface S is given by

$$\overline{\lambda}(\phi) = \lambda(\phi)^g.$$

For fixed g, $\overline{\lambda}$ is bounded below by a constant greater than one, and the minimum genus-normalized dilatations $(\delta_g)^g$ are bounded from above by a constant independent of g [32]. The smallest known accumulation point of genus-normalized dilatations is

$$\ell_0 = \frac{3 + \sqrt{5}}{2} = 1 + \text{golden mean} \tag{1}$$

[14] (see also [1] [21]).

In [38], Thurston defined orientable pseudo-Anosov mapping classes associated to bipartite classical Coxeter graphs. For these examples the homological dilatation is bounded below by Lehmer's number $\lambda_L \approx 1.17628$ [25]. By contrast, for mixed-sign Coxeter mapping classes the dilatations can be arbitrarily close to one. Let ℓ_0 be the accumulation point given in Equation (1).

The *house* $|p|$ of a polynomial $p(x)$ is given by

$$|p| = \min\{|x| \ : \ p(x) = 1\}.$$

Consider the polynomial

$$LT_g = x^{2g} - x^{g+1} - x^g - x^{g-1} + 1.$$

This sequence of polynomials has the property that

$$\lim_{g \to \infty} |LT_g| = \ell_0.$$

In [24], Lanneau and Thiffeault ask whether the following is true:

Question 1.3 (Lanneau-Thiffeault) *Is it true that the minimum dilatation for orientable pseudo-Anosov mapping classes on a closed surfaces of genus g equals $|LT_g|$ for all even g?*

From our proof of Theorem 1.2 we obtain the following.

Theorem 1.4 *An affirmative answer to Question 1.3 implies that for an infinite number of g, the minimum dilatation of orientable pseudo-Anosov mapping classes on a closed surface of genus g is realized by a mixed-sign Coxeter mapping class.*

Outline of Paper. Let Γ be a (simply-laced) Coxeter graph with vertices $\mathcal{V}$ and edges $\mathcal{E}$. A *sign-labeling* on $\mathcal{V}$ is a map

$$\mathfrak{s} : \mathcal{V} \to \{+1, -1\}.$$

The pair $(\Gamma, \mathfrak{s})$ is called a *mixed-sign Coxeter graph.*

Let $\mathcal{V} = \{v_1, \dots, v_k\}$ be an ordering on $\mathcal{V}$, and let $A_\Gamma = [a_{i,j}]$ be the adjacency matrix for Γ, that is,

$$a_{i,j} = \begin{cases} 1 & \text{if } v_i \text{ and } v_j \text{ are adjacent, and} \\ 0 & \text{otherwise.} \end{cases}$$

A *fatgraph structure* on Γ is a cyclic ordering on the set of adjacent vertices $\mathcal{V}_v$ for each vertex v of Γ. A graph Γ with such a structure is called a *fatgraph.*

In Section 2, we construct the following objects from an ordered mixed-sign Coxeter fatgraph $(\Gamma, \mathfrak{s})$:

1. a mapping class $(S_\Gamma, \phi_{\Gamma,\mathfrak{s}})$, where S_Γ is a compact oriented surface of finite type;
2. a generalized Coxeter reflection group $(\mathcal{W}_{\Gamma,\mathfrak{s}}, \mathcal{R}_{\Gamma,\mathfrak{s}})$ and Coxeter element $\omega_{\Gamma,\mathfrak{s}}$; and
3. a symplectic representation of an Artin group $\rho_\Gamma : \mathcal{A}_\Gamma \to GL(\mathbb{R}^{\mathcal{V}})$.

The surface S_Γ does not depend on $\mathfrak{s}$ and is determined up to homeomorphism by the existence of a set of essential simple closed curves $\mathcal{C}_\Gamma = \{\gamma_1, \dots, \gamma_k\} \subset S_\Gamma$ associated to the ordered vertices of Γ with the following properties:

(i) for $1 \leq i < j \leq k$, we have

$$\iota_{\mathrm{alg}}([\gamma_i], [\gamma_j]) = \iota_{\mathrm{geo}}(\gamma_i, \gamma_j) = a_{i,j};$$

(ii) for any fixed i, the cyclic order of the intersections of γ_i with the remaining γ_j determined by the orientation on γ_i is compatible with the fatgraph ordering of $\mathcal{V}_{v_i}$; and

(iii) S_Γ has a deformation retract to the union $\bigcup_{i=1}^{k} \gamma_i$, in other words, the union forms a *spine* for S_Γ.

The pair $(S_\Gamma, \mathcal{C}_\Gamma)$ is called the *(oriented) geometric realization* of the ordered fatgraph Γ. The *mixed-sign Coxeter mapping class* $(S_\Gamma, \phi_{\Gamma,\mathfrak{s}})$ is the mapping class defined as a product of Dehn twists

$$\phi_{\Gamma,\mathfrak{s}} = (\delta_1)^{\mathfrak{s}(1)} \cdots (\delta_k)^{\mathfrak{s}(k)},$$

where δ_i is the positive (or right) Dehn twist centered at γ_i, for $i = 1, \dots, k$.

We give a sufficient condition (Theorem 2.14) on $(\Gamma, \mathfrak{s})$ for $(S_{\Gamma,\mathfrak{s}}, \phi_{\Gamma,\mathfrak{s}})$ to be pseudo-Anosov in terms of the generalized Coxeter element $\omega_{\Gamma,\mathfrak{s}}$ of $(\mathcal{W}_{\Gamma,\mathfrak{s}}, \mathcal{R}_{\Gamma,\mathfrak{s}})$, and show that the homological dilatation of $\phi_{\Gamma,\mathfrak{s}}$ and the spectral radius of the generalized Coxeter element $\omega_{\Gamma,\mathfrak{s}}$ are equal (Theorem 2.13).

In Section 3, we define a general operation on mapping classes called twisting. For mixed-sign Coxeter mapping classes, this amounts to inductively joining certain graphs called twist graphs to the defining graph of a mapping class. In [14] we found a collection of mapping classes on closed surfaces

$$\mathcal{C} = \{(S_g, \phi_g) \ : \ g = 2 \text{ or } 4 \pmod 6\}$$

so that $\lambda(\phi_g) = |LT_g|$ for all g. To prove the main theorem, we realize an infinite subcollection of $\mathcal{C}$ as closures of mixed-sign Coxeter mapping classes.

Acknowledgments: I am grateful to the Tokyo Institute of Technology and University of Tokyo for their support during the writing of this paper.

2 Mixed-sign Coxeter systems and associated mapping classes.

In this section, we define from an ordered mixed-sign Coxeter graph $(\Gamma, \mathfrak{s})$ a reflection group $\mathcal{W}_{\Gamma,\mathfrak{s}}$ (Section 2.1)), and a representation of the Artin group $\mathcal{A}_\Gamma$

$$\rho_\Gamma : \mathcal{A}_\Gamma \to GL(\mathbb{R}^{\mathcal{V}})$$

(Section 2.2). When Γ is given a fatgraph structure, we define an associated geometric realization $(S_\Gamma, \mathcal{C}_\Gamma)$ of Γ, and a mapping class $\phi_{\Gamma,\mathfrak{s}} : S_\Gamma \to S_\Gamma$ (Section 2.3). The groups $\mathcal{A}_\Gamma$ and $\mathcal{W}_{\Gamma,\mathfrak{s}}$ come with k standard generators $\{\sigma_1, \dots, \sigma_k\}$ and $\{s_1, \dots, s_k\}$, respectively. Let σ and w be the epimorphisms of the free group $\langle x_1, \dots, x_k\rangle$ to $\mathcal{A}_\Gamma$ and $\mathcal{W}_{\Gamma,\mathfrak{s}}$, where $\sigma(x_i) = \sigma_i$ and $w(x_i) = s_i$.

$$\begin{tikzcd}
\langle x_1, \dots, x_k\rangle \arrow[r, "\sigma"] \arrow[dr, "w"] & \mathcal{A}_\Gamma \arrow[r, "\rho_\Gamma"] & GL(\mathbb{R}^{\mathcal{V}}) \arrow[r, "\eta"] & GL(H_1(S_\Gamma; \mathbb{R})) \\
& \mathcal{W}_{\Gamma,\mathfrak{s}} \arrow[r, "\subset"] & GL(\mathbb{R}^{\mathcal{V}}).
\end{tikzcd}$$

Let $\omega_{\Gamma,\mathfrak{s}} = w(x_1 \cdots x_k)$, called the *(mixed-sign) Coxeter element.* Write $\mathfrak{s}(i) = \mathfrak{s}(v_i)$, and let $\sigma_{\Gamma,\mathfrak{s}} = \rho_\Gamma(\sigma_1^{\mathfrak{s}(1)} \cdots \sigma_k^{\mathfrak{s}(k)})$. The representations ρ_Γ and η preserve symplectic forms, while the elements of $\mathcal{W}_{\Gamma,\mathfrak{s}}$ preserve an orthogonal one, but we will show

$$\omega_{\Gamma,\mathfrak{s}} = -\sigma_{\Gamma,\mathfrak{s}}$$

as elements of $GL(\mathbb{R}^{\mathcal{V}})$ (Theorem 2.6). The element $\sigma_{\Gamma,\mathfrak{s}}$ satisfies

$$\eta(\rho_\Gamma(\sigma_{\Gamma,\mathfrak{s}})) = (\phi_{\Gamma,\mathfrak{s}})_*$$

and hence the homological dilatation of $\phi_{\Gamma,\mathfrak{s}}$ and the spectral radius of the Coxeter element $\omega_{\Gamma,\mathfrak{s}}$ satisfy

$$\lambda_{\text{hom}}(\phi_{\Gamma,\mathfrak{s}}) = |\omega_{\Gamma,\mathfrak{s}}|.$$

(Theorem 2.13). From this we derive a sufficient condition for a mixed-sign Coxeter mapping class to be pseudo-Anosov (Theorem 2.14).

The following table summarizes the defining data for the main objects in this section.

Data	**Object**	**Notation**
$\Gamma, \mathfrak{s}$	Coxeter system	$(\mathcal{W}_{\Gamma,\mathfrak{s}}, \mathcal{R}_{\Gamma,\mathfrak{s}})$
ordered $\Gamma, \mathfrak{s}$	Coxeter element	$\omega_{\Gamma,\mathfrak{s}}$
Γ	Artin group	$\mathcal{A}_\Gamma$
ordered Γ	Artin group representation	$\rho_\Gamma : \mathcal{A}_\Gamma \to GL(\mathbb{R}^{\mathcal{V}})$
ordered fatgraph Γ	geometric realization	$(S_\Gamma, \mathcal{C}_\Gamma)$
ordered fatgraph $\Gamma, \mathfrak{s}$	Coxeter mapping class	$(S_\Gamma, \phi_{\Gamma,\mathfrak{s}})$

Mixed-sign Coxeter mapping classes are defined on surfaces with boundary, but in some cases the dynamical information contained in the mapping class extends to the closure of the surface obtained by filling in disks. This is discussed in Section 2.4. The special case of mapping classes associated to bipartite Coxeter graphs is treated in Section 2.5. Section 2.6 contains examples of minimum dilatation orientable pseudo-Anosov mapping classes for small genus.

Remark 2.1 The study of mapping classes using Coxeter graphs and associated reflection groups has a long history in algebraic geometry dating back to the 19th century, particularly in the study of complex surface singularities (see, for example, [35], [10] and references therein). The focus in geometric topology has on the other hand been on representations of the Artin group of a Coxeter graph into the mapping class group. The difference comes from the fact the associated bilinear forms left invariant by the respective automorphism groups are different: one being symmetric and the other symplectic. From this point of view our results concerning special elements of the Artin group, and Coxeter elements of the Coxeter reflection group are part of an overlap in the two theories (see also [40] [16] [17]).

2.1 Mixed-sign Coxeter reflection group

In this section we define mixed-sign Coxeter systems.

Let $(\Gamma, \mathfrak{s})$ be an ordered mixed-sign Coxeter graph with vertices $\mathcal{V} = \{v_1, \dots, v_n\}$. For $i, j = 1, \dots, k$, define

$$m_{i,j} = \begin{cases} 1 & \text{if } i = j \\ 2 & \text{if } v_i \text{ and } v_j \text{ are not connected by an edge} \\ 3 & \text{if } v_i \text{ and } v_j \text{ are connected by an edge.} \end{cases}$$

Remark 2.2 For the classical definition of Coxeter and Artin groups, the $m_{i,j}$ are allowed to vary (for $i \neq j$) in the set $\{2, 3, \dots, \infty\}$. In this paper, we restrict only to the simply-laced case described above.

Let $I_{\mathfrak{s}}$ be the $n \times n$ matrix with 0 on the off-diagonal, and diagonal entries equal to $\mathfrak{s}(1), \dots, \mathfrak{s}(n)$. Let $A = [a_{i,j}]$ be the adjacency matrix of Γ, A^+ the upper triangular part of A, and $U = I_{\mathfrak{s}} - A^+$. Then U determines a symmetric form

$$B = U + U^T$$

on V.

The Coxeter system $(\mathcal{W}, \mathcal{R}) = (\mathcal{W}_{\Gamma,\mathfrak{s}}, \mathcal{R}_{\Gamma,\mathfrak{s}})$ associated to $(\Gamma, \mathfrak{s})$ is the subgroup of $\mathrm{GL}(\mathbb{R}^{\mathcal{V}})$ generated by $\mathcal{R}_{\Gamma,\mathfrak{s}} = \{s_1, \dots, s_n\}$, where the s_i are defined by

$$\begin{aligned} s_i(v_j) &= v_j - 2\frac{B(v_i, v_j)}{B(v_I, v_I)} v_i \\ &= \begin{cases} -v_j & \text{if } i = j, \\ v_j + \mathfrak{s}(i) a_{i,j} v_i & \text{if } i \neq j. \end{cases} \end{aligned}$$

Each s_i can be interpreted as a reflection through the hyperplane perpendicular to v_i in $\mathbb{R}^{\mathcal{V}}$ with respect to the symmetric form B. If $\mathfrak{s} \equiv 1$, then $(\mathcal{W}, \mathcal{S})$ is the classical Coxeter system.

Given a mixed-sign ordered Coxeter graph $(\Gamma, \mathfrak{s})$, we define the *Coxeter element* to be

$$\omega_{\Gamma,\mathfrak{s}} = s_1 \cdots s_n \in \mathcal{W}_{\Gamma,\mathfrak{s}}.$$

Coxeter systems $(\mathcal{W},\mathcal{R})$, and more generally reflection systems, are classified by the type of associated bilinear form B. If B is positive or negative definite, we say $(\mathcal{W},\mathcal{R})$ is *spherical*, if B is positive or negative semi-definite, then we say $(\mathcal{W},\mathcal{R})$ is *affine*, and otherwise, we say $(\mathcal{W},\mathcal{R})$ is *higher rank*. (see [19]).

The classical (simply-laced) Coxeter systems $(\mathcal{W},\mathcal{R})$ and their Coxeter elements ω_Γ, where $\mathfrak{s} \equiv 1$, have the following special properties (see, for example, [5] [2] [29]).

(i) (*Presentation.*) The Coxeter group $\mathcal{W}$ has presentation in terms of the standard generators $\mathcal{R} = \{s_1, \dots, s_k\}$:

$$\langle s_1, \dots, s_k \ : \ (s_i s_j)^{m_{i,j}} \rangle.$$

(ii) (*Monotonicity.*) The spectral radius of Coxeter elements is monotone increasing with respect to inclusion of Coxeter graphs that respect ordering.

(iii) (*Bipartite Coxeter eigenvalue.*) The spectral radius of Coxeter elements is bounded from below by

$$\frac{(\mu^2-2)+\sqrt{(\mu^2-2)^2-4}}{2},$$

known as the *bipartite eigenvalue* of the Coxeter system.

These properties do not necessarily hold for mixed-sign Coxeter systems.

Example 2.3 If v_i and v_j are two adjacent vertices on Γ, and $\mathfrak{s}(i) \neq \mathfrak{s}(j)$, then $s_i s_j$ has infinite order.

Example 2.4 The mixed-sign Coxeter graph $(\Gamma, \mathfrak{s})$, where Γ is the complete graph on 3 vertices, and $\mathfrak{s} \equiv -1$, is spherical. The Coxeter group is isomorphic to the symmetric group on 4 letters, while the three generator group with only the pairwise relations is isomorphic to the affine group associated to $\widetilde{A}_2 = (\Gamma, +1)$ and has infinite order.

Example 2.5 Property (ii), the monotonicity property, of classical Coxeter elements implies that there is a lower bound greater than 1 for the spectral radius of classical Coxeter elements of non-spherical or affine Coxeter graphs. For classical Coxeter elements with $\mu^2 > 2$, the smallest positive spectral radius is Lehmer's number

$$\lambda_L \approx 1.17628$$

(see [29]), which is also the smallest possible bipartite eigenvalue of a non-spherical and non-affine Coxeter graph. On the other hand, as we see later in this paper, the spectral radius of mixed-sign Coxeter elements can be made arbitrarily close to one.

2.2 Representations of Artin groups

In this section we recall the definition of the Artin group $\mathcal{A}_\Gamma$ associated to a Coxeter graph Γ, and define representations of $\mathcal{A}_\Gamma$ associated to an ordered mixed-sign Coxeter graph $(\Gamma, \mathfrak{s})$.

The *Artin group* of Γ is the group

$$\mathcal{A}_\Gamma = \langle \sigma_1, \dots, \sigma_n \ : \ [\sigma_i \sigma_j]_{m_{i,j}} = [\sigma_j \sigma_i]_{m_{i,j}} \rangle$$

where $[\sigma_i \sigma_j]_m$ is the alternating product

$$[\sigma_i \sigma_j]_m = \sigma_i \sigma_j \sigma_i \dots$$

of length m. If Γ is the classical Coxeter graph A_n, then $\mathcal{A}_\Gamma$ is the braid group on the disk with $n+1$ punctures (see, e.g., [4]). The definition of Artin group does not depend on the ordering on $\mathcal{V}$.

Let $\mathbb{R}^{\mathcal{V}}$ be the vector space of real labels on the vertices of Γ. The ordered vertices $\mathcal{V}$ determine an ordered basis $v_1, \dots, v_n$ of $\mathbb{R}^{\mathcal{V}}$. Let A be the adjacency matrix for Γ. Let F be the skew-symmetric bilinear form on $\mathbb{R}^{\mathcal{V}}$ defined with respect to $v_1, \dots, v_n$ by

$$F = A^+ - A^-,$$

where A^+ is the upper triangular part of A, and A^- is the lower triangular part. The matrix F defines a skew symmetric form on $\mathbb{R}^{\mathcal{V}}$ that depends on the choice of ordering of $\mathcal{V}$.

Let $\mathfrak{s}$ be a sign-labeling for Γ. Define ρ_Γ to be the representation

$$\rho_\Gamma : \mathcal{A}_\Gamma \to \mathrm{GL}(\mathbb{R}^{\mathcal{V}})$$

preserving F defined by

$$\begin{aligned} \rho_\Gamma(\sigma_i)(v_j) &= v_j + F(v_i, v_j) v_i \\ &= \begin{cases} v_j & \text{if } i = j, \\ v_j + a_{i,j} v_i & \text{if } i < j, \\ v_j - a_{i,j} v_i & \text{if } i > j. \end{cases} \end{aligned}$$

Then the image preserves F. We call ρ_Γ the *Artin representation* of $\mathcal{A}_\Gamma$. Define

$$\sigma_{\Gamma,\mathfrak{s}} = \sigma_1^{\mathfrak{s}(1)} \cdots \sigma_k^{\mathfrak{s}(k)}$$

to be the *Artin element* associated to the ordered mixed-sign Coxeter graph.

Theorem 2.6 *The Coxeter element $\omega_{\Gamma,\mathfrak{s}}$ and the Artin element $\sigma_{\Gamma,\mathfrak{s}}$ are related by*

$$\omega_{\Gamma,\mathfrak{s}} = -\rho_\Gamma(\sigma_{\Gamma,\mathfrak{s}}).$$

Let $B_c = U + cU^T$, for $c \in \mathbb{C} \setminus 0$. Then we have $B = B_1$ and $F = B_{-1}$. Now define elements $f_1^{(c)}, \ldots, f_n^{(c)} \in \mathrm{GL}(\mathbb{R}^{\mathcal{V}})$ by

$$\begin{aligned} f_i^{(c)}(v_j) &= v_j - \mathfrak{s}(i) B_c(i,j) v_i \\ &= \begin{cases} -cv_i & \text{if } i = j \\ v_j + \mathfrak{s}(i) a_{i,j} v_i & \text{if } i < j \\ v_j + c\mathfrak{s}(i) a_{i,j} v_i & \text{if } i > j \end{cases} \end{aligned}$$

Then $f_i^{(1)} = s_i$ and $f_i^{(-1)} = \rho_\Gamma(\sigma_i^{\mathfrak{s}(i)})$.

Theorem 2.6 follows from the following generalization of a result of Howlett [18].

Lemma 2.7 *Using the above notation*

$$f_1^c \cdots f_n^c = -cU^{-1}U^T.$$

We present the generalized proof here.

Proof of Lemma 2.7. First we notice that

$$\begin{aligned} Uf_1^{(c)} &= \begin{bmatrix} \mathfrak{s}(1) & -a_{1,2} & -a_{1,3} & \ldots & -a_{1,n} \\ 0 & \mathfrak{s}(1) & -a_{2,3} & \ldots & -a_{2,n} \\ \ldots & & & & \\ 0 & & & \ldots & \mathfrak{s}(n) \end{bmatrix} \begin{bmatrix} -c & \mathfrak{s}(1)a_{1,2} & & \ldots & \mathfrak{s}(1)a_{1,n} \\ 0 & 1 & 0 & \ldots & 0 \\ \ldots & & & & \\ 0 & & & & 1 \end{bmatrix} \\ &= \begin{bmatrix} -c\mathfrak{s}(1) & 0 & & \ldots & 0 \\ 0 & \mathfrak{s}(1) & -a_{2,3} & \ldots & -a_{2,n} \\ \ldots & & & & \\ 0 & & & \ldots & \mathfrak{s}(n) \end{bmatrix} \end{aligned}$$

Assume that

$$\begin{aligned} Uf_1^{(c)} \cdots f_k^{(c)} &= \begin{bmatrix} -c\mathfrak{s}(1) & 0 & & & \ldots & & & 0 \\ -ca_{1,2} & -c\mathfrak{s}(1) & 0 & & & & \ldots & 0 \\ & \ldots & & & & & & \\ -ca_{k,1} & \ldots & -ca_{k,k-1} & -c\mathfrak{s}(k) & 0 & & \ldots & 0 \\ 0 & & \ldots & 0 & \mathfrak{s}(k+1) & -a_{k+1,k+2} & \ldots & -a_{k+1,n} \\ & \ldots & & & & & & \\ 0 & & & \ldots & & 0 & \mathfrak{s}(n-1) & -a_{n-1,n} \\ 0 & & & \ldots & & & 0 & \mathfrak{s}(n) \end{bmatrix} \\ &= \begin{bmatrix} L_k & 0 \\ 0 & U_k \end{bmatrix}. \end{aligned}$$

Multiplying on the right by

$$f_{k+1}^{(c)} = \left[\begin{array}{c|c|c} I & 0 & 0 \\ \hline -\mathfrak{s}(k+1)ca_{k+1,1} \cdots - \mathfrak{s}(k+1)ca_{k+1,k} & -c & \mathfrak{s}(k+1)a_{k+1,k+2} \ldots \mathfrak{s}(k+1)a_{k+1,n} \\ \hline 0 & 0 & I \end{array} \right]$$

amounts to replacing the $k+1$st row of $Uf_1^{(c)} \cdots f_k^{(c)}$ by

$$[a_{k+1,1}, \ldots, a_{k+1,k}, -\mathfrak{s}(k+1), 0, \ldots, 0].$$

Thus,

$$Uf_1^{(c)} \cdots f_{k+1}^{(c)} = \begin{bmatrix} L_{k+1} & 0 \\ 0 & U_{k+1} \end{bmatrix}$$

and $L_n = -cU^T$ as desired. □

For each c, the transformation $f = f_1^{(c)} \cdots f_n^{(c)}$ satisfies

$$f^T B_c f = B_c.$$

The following consequence of Lemma 2.7 completes the proof of Theorem 2.6.

Theorem 2.8 *The mixed-sign Coxeter element and representation of the corresponding element of the Artin group is given by*

$$\omega_{\Gamma,\mathfrak{s}} = -U^{-1}U^T,$$

and

$$\rho_\Gamma(\sigma_{\Gamma,\mathfrak{s}}) = U^{-1}U^T.$$

2.3 Geometric realization and mixed-sign Coxeter mapping class

In this section, we define a compact oriented surface S_Γ from an ordered Coxeter fatgraph Γ, and a mapping class $\phi_{\Gamma,\mathfrak{s}}$ from Γ and a sign-labeling s.

Let

$$\mathfrak{o} : \mathcal{V} \to \{1, \ldots, n\}$$

be the bijection corresponding to the ordering on $\mathcal{V}$, and let

$$\mathfrak{o}_v : \mathcal{V}_v \to \{1, \ldots, \deg(v)\}$$

be a bijection (determined once one chooses the value at a single vertex) defined on the adjacent vertices $\mathcal{V}_v$ of each vertex $v \in \mathcal{V}$ compatible with the fatgraph structure of Γ. Construct a system of oriented annuli T_v with core curve γ_v for $v \in \mathcal{V}$, so that

1. T_v and T_w are glued together along a square patch if and only if v and w are connected by an edge;
2. if $\mathfrak{o}(v) < \mathfrak{o}(w)$, then $i_{\mathrm{alg}}(\gamma_v, \gamma_w) > 0$; and
3. If v is a vertex, then for each of the the core curves γ_w, for $w \in \mathcal{V}_v$, intersect γ_v in a cyclic ordering that respects the orientation of ℓ_v and the cyclic ordering $\mathfrak{o}_v$.

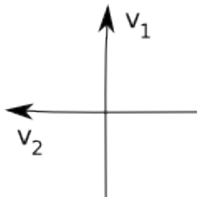

Figure 1: Positive intersection

Here we use the convention that if γ_i and γ_j intersect as in Figure 1, then $i_{\mathrm{alg}}(\gamma_i, \gamma_j) = 1$.

Figure 2 shows the arrangement of $T_{v_1}, T_{v_2}, T_{v_3}$ and T_v where

(a) $\mathfrak{o}_v(v_1) < \mathfrak{o}_v(v_2) < \mathfrak{o}_v(v_3)$,

(b) $\mathfrak{o}(v) < \mathfrak{o}(v_1), \mathfrak{o}(v_3)$, and

(c) $\mathfrak{o}(v) > \mathfrak{o}(v_2)$.

The arrows in the figure indicate which vertex comes before the other in the global ordering. One sees that the surface depends on the relative global ordering of adjacent vertices and the fatgraph structure.

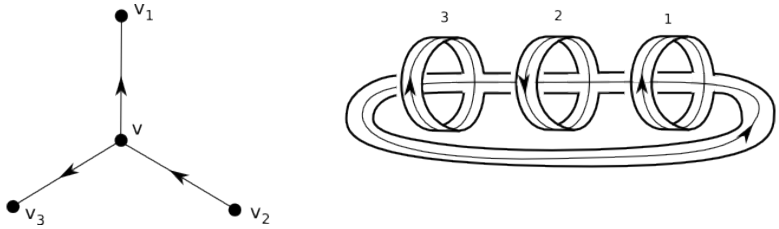

Figure 2: A local picture of Coxeter graph and corresponding union of annuli

Let $\mathfrak{s}$ be a sign-labeling for Γ. Let $\phi_{\Gamma,\mathfrak{s}} S_\Gamma \to S_\Gamma$ be the mapping class defined by

$$\phi_{\Gamma,\mathfrak{s}} = (\delta_1)^{\mathfrak{s}(1)} \cdots (\delta_k)^{\mathfrak{s}(k)},$$

where δ_i are the right Dehn twists centered at γ_i. Then $(S_\Gamma, \phi_{\Gamma,\mathfrak{s}})$ is the *Coxeter mapping class* associated to $(\Gamma, \mathfrak{s})$.

Remark 2.9 There is a natural way to embed S_Γ in the three sphere S^3 so that the annuli are twisted with a left or right twist according to the sign of the corresponding vertex on $(\Gamma, \mathfrak{s})$. Then the image of S_Γ is a Seifert surface for the knot or link L given by the image of the boundary of S_Γ. Under extra conditions, for example, if Γ is a tree, L is a fibered link with fiber $S_{\Gamma,\mathfrak{s}}$ and $\phi_{\Gamma,\mathfrak{s}}$ is the monodromy of the fibration [13].

Lemma 2.10 *The surfaces* S_Γ *depend only on the choice of ordering and fatgraph structure on* Γ*. Different orderings and fatgraph structures can give rise to different homeomorphism types of surfaces.*

By contrast, the topological Euler characteristic of S_Γ is independent of the ordering and fatgraph structure.

Lemma 2.11 *Let S_Γ be a geometric realization of Γ. Then $\chi(S_\Gamma) = -|\mathcal{E}|$, where $|\mathcal{E}|$ is the total number of edges of Γ. In particular, $\chi(S_\Gamma)$ does not depend on the ordering of $\mathcal{V}$ or the fatgraph structure.*

Proof. The construction of S_Γ is inductive with respect to an ordering on the vertices $\mathcal{V} = \{v_1, \dots, v_k\}$. At each stage i we attach an annulus to the preceding surface along patches one for each vertex v_j adjacent to v_i such that $j < i$. The Euler characteristic thus changes by the number of such vertices. Thus each edge is counted exactly once. $\square$

Remark 2.12 We could extend the definition of $(S_\Gamma, \phi_{\Gamma,\mathfrak{s}})$, by replacing $\mathfrak{s}$ with

$$\epsilon : \mathcal{V} \to \mathbb{Z}^*,$$

where $\mathbb{Z}^*$ is the set of nonzero integers, and setting

$$\phi_{\Gamma,\epsilon} = \delta_1^{\epsilon_1} \circ \cdots \circ \delta_n^{\epsilon_n}.$$

Each $\phi_{\Gamma,\epsilon}$ is, however, also associated to a signed graph. The signed graph $(\Gamma', \mathfrak{s})$ is obtained from (Γ, ϵ) by successively replacing each vertex v_i in Γ with $m_i = |\epsilon_n|$ copies $v_i^{(j)}$. Each of the new vertices $v_i^{(j)}$ of Γ' has edges connecting it to all the vertices to which v_i was connected. The new sign labels on $v_i^{(j)}$ equal the sign of ϵ.

Let $\mathbb{R}^{\mathcal{V}} \hookrightarrow H_1(S_\Gamma; \mathbb{R})$ be the linear map defined by sending the ith basis vector to $[\gamma_i]$. Let $GL(\mathbb{R}^{\mathcal{V}}) \to GL(H_1(S_\Gamma; \mathbb{R}))$ be the homomorphism defined by extending by the identity on the complementary space of the image of $\mathbb{R}^{\mathcal{V}}$.

Theorem 2.13 *The induced map $(\phi_{\Gamma,\mathfrak{s}})_* : H_1(S_\Gamma; \mathbb{R}) \to H_1(S_\Gamma; \mathbb{R})$ on homology satisfies*

$$(\phi_{\Gamma,\mathfrak{s}})_* = \rho_\Gamma(\sigma_{\Gamma,\mathfrak{s}})$$

and hence

$$\lambda_{hom}(\phi_{\Gamma,\mathfrak{s}}) = |\omega_{\Gamma,\mathfrak{s}}|.$$

Proof. Let $g_i = [\gamma_i]$ be the homology classes. The choice of orientations and algebraic intersections of $g_1, \dots, g_k$ satisfy

$$(\delta_i)_*(g_j^{\mathfrak{s}(i)} = \begin{cases} g_j & \text{if } i = j \\ g_j + \mathfrak{s}(i) g_i & \text{if } i < j \\ g_j - \mathfrak{s}(i) g_i & \text{if } i > j. \end{cases}$$

Thus, $(\delta_i)_*^{\mathfrak{s}(i)}$ restricted to the image of $\mathbb{R}^{\mathcal{V}}$ in $H_1(S_\Gamma; \mathbb{R})$ equals $\rho_\Gamma(\sigma_i)$. $\square$

Theorem 2.14 *If* Γ *is connected and the spectral radius of the Coxeter element* $|\omega_{\Gamma,\mathfrak{s}}|$ *is greater than one, then* $(S_{\Gamma,\mathfrak{s}}, \phi_{\Gamma,\mathfrak{s}})$ *is pseudo-Anosov, and the dilatation satisfies*

$$\lambda(\phi_{\Gamma,\mathfrak{s}}) \geq |\omega_{\Gamma,\mathfrak{s}}|.$$

Proof. By the Nielsen-Thurston classification, any mapping class is either periodic, reducible or pseudo-Anosov [38]. Since Γ is connected, ω_Γ is irreducible, and hence so is the homological action of ϕ_Γ. This implies that ϕ_Γ is not reducible.

Since $\lambda_{\text{hom}}(\phi_{\Gamma,\mathfrak{s}}) > 1$, $\phi_{\Gamma,\mathfrak{s}}$ is not periodic, so it must be pseudo-Anosov. The rest follows from the following well-known inequality (see, e.g. [34]).

$$\lambda_{\text{hom}}(\phi) \leq \lambda_{\text{geo}}(\phi).$$

□

2.4 Mapping classes on closures and interiors

Let S be a compact surface, we have defined the mapping class group $\text{Mod}(S)$ to be the group of isotopy classes of orientation preserving self-homeomorphisms of S up to isotopy relative to the boundary of S. Consider the interior $\text{int}(S)$ of S. Topologically, this is homeomorphic to a surface with punctures one for each boundary component of S. Let $\text{Mod}(\text{int}(S))$ be the group of orientation preserving self-homeomorphisms on $\text{int}(S)$ modulo isotopy. Then the map

$$\alpha : \text{Mod}(S) \to \text{Mod}(\text{int}(S)) \tag{2}$$

defined by restriction has kernel generated by Dehn twists centered at boundary parallel simple closed curves. Note that the homomorphism in (2) is not onto, since elements of $\text{Mod}(\text{int}(S))$ only preserve the punctures of $\text{int}(S)$ as a set, while elements of $\text{Mod}(S)$ preserve the boundary components.

The following results are well-known, and are contained for example in [4].

Lemma 2.15 *If* (S, ϕ) *is a pseudo-Anosov element of Mod*(S)*, then* $\alpha(S, \phi)$ *is also pseudo-Anosov, and the dilatations are the same.*

Proof. If (S, ϕ) is pseudo-Anosov, and $(\mathcal{F}^\pm, \nu^\pm)$ are its associated stable and unstable foliations, then $(\mathcal{F}^\pm, \nu^\pm)$ also define stable and unstable foliations for $\alpha(S, \phi)$, and the stretching factor λ is also preserved. □

Let $\overline{S}$ be the closed surface obtained by filling in the boundary components of S with disks. Then there is a homomorphism

$$\beta : \text{Mod}(S) \to \text{Mod}(\overline{S}) \tag{3}$$

defined by extending over disks. This map is neither one-to-one nor onto. Furthermore, the image of a pseudo-Anosov mapping class is not necessary pseudo-Anosov. We will write $(\overline{S}, \overline{\phi}) = \beta(S, \phi)$.

Lemma 2.16 *If* (S,ϕ) *is pseudo-Anosov, and none of the boundary components are 1-pronged, then* $(\overline{S},\overline{\phi})$ *is also pseudo-Anosov with dilatation* $\lambda(\overline{\phi}) = \lambda(\phi)$.

The idea of the proof is that if there are no 1-pronged boundary components, then the stable and unstable foliations of (S,ϕ) determine invariant transverse measured foliations for $\overline{\phi}$ with expansion factor $\lambda^{\pm 1}$ for $\lambda = \lambda(\phi)$ (see, for example, [15], Lemma 2.5).

We can also refine Lemma 2.16 as follows. Let (S,ϕ) be a mapping class, where S is compact. For any boundary component b of S, let $b = b_1,\dots,b_s$ be the orbit of b under the action of ϕ. Let $cl(S,b)$ be the surface obtained by filling in the boundary components $b_1,\dots,b_s$ with disks, and let $cl(\phi,b)$ be the extension of ϕ. Let $cl(S,\phi,b) = (cl(S,b), cl(\phi,b))$. If (S,ϕ) is pseudo-Anosov, and b is m-pronged, then all orbits of b are also m-pronged.

Lemma 2.17 *If* (S,ϕ) *is pseudo-Anosov, then* $(cl(S,b), cl(\phi,b))$ *is pseudo-Anosov if the boundary components* $b_1,\dots,b_s$ *are not 1-pronged. In this case,*

$$\lambda(cl(\phi)) = \lambda(\phi).$$

The proof is the same as for Lemma 2.16.

2.5 Bipartite graphs

In this section we collect some special properties of mixed-sign Coxeter systems, and mixed-sign Coxeter mapping classes associated to bipartite graphs.

A Coxeter graph Γ is *bipartite (with bipartite ordering)* if

(i) its vertices can be separated into two disjoint sets $\mathcal{V} = \mathcal{V}_1 \cup \mathcal{V}_2$ where the subgraph of Γ generated by $\mathcal{V}_i$ has no edges for $i = 1, 2$; and

(ii) by the ordering on $\mathcal{V}$ has the property that the elements of $\mathcal{V}_1$ proceed all the elements of $\mathcal{V}_2$.

A graph Γ is bipartite if and only if it contains no odd cycles. Given a sign-labeling $\mathfrak{s}$ of a Coxeter graph Γ. Let $\bar{\mathfrak{s}}$ be the sign-labeling defined by $\bar{\mathfrak{s}}(v) = -\mathfrak{s}(v)$ for all $v \in \mathcal{V}$.

Theorem 2.18 *If* Γ *is bipartite, and* $\mathfrak{s}$ *is any sign-labeling on* Γ*, then* $(\mathcal{W}_{\Gamma,\mathfrak{s}}, \mathcal{R}_{\Gamma,\mathfrak{s}})$ *and* $(\mathcal{W}_{\Gamma,\bar{\mathfrak{s}}}, \mathcal{R}_{\Gamma,\bar{\mathfrak{s}}})$ *are conjugate as subgroups of* $GL(\mathcal{R}^{\mathcal{V}})$*, and, in particular, the spectral radius of Coxeter elements satisfies*

$$|\omega_{\Gamma,\mathfrak{s}}| = |\omega_{\Gamma,\bar{\mathfrak{s}}}|.$$

Proof. It suffices to show that the generating sets $\mathcal{R}_{\Gamma,\mathfrak{s}} = \{s_1, \dots, s_k\}$ and $\mathcal{R}_{\Gamma,\bar{\mathfrak{s}}} = \{\overline{s}_1, \dots, \overline{s}_k\}$ are conjugate as elements of $GL(\mathbb{R}^{\mathcal{V}})$.

let $\mathcal{V} = \mathcal{V}_1 \cup \mathcal{V}_2$ be the bipartite partition. Let k_i be the number elements in $\mathcal{V}_i$, for $i = 1, 2$, and let $k = k_1 + k_2$ be the total number of vertices $\mathcal{V}$. Let I_{k_1,k_2} be the $k \times k$ diagonal matrix with the first k_1 diagonal entries equal to 1 and the second k_2 diagonal entries equal to -1. Then s_i and s_i' satisfy

$$s_i = I_{k_1,k_2} \overline{s}_i I_{k_1,k_2}.$$

□

If a graph Γ is bipartite, and is given the bipartite ordering, then there is a fatgraph structure on Γ so that after cutting each annulus at a transversal arc between the two boundary components, the surface can be placed on a plane as a union of rectangles oriented in vertical and horizontal directions as in Figure 3. The right diagram in Figure 3 gives the corresponding surface S_Γ.

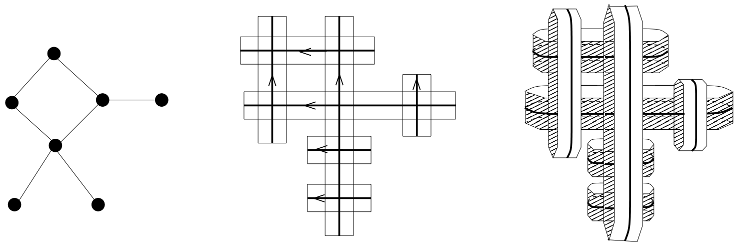

Figure 3: Surface associated to a bipartite graph

The *bipartite eigenvalue* of a graph Γ is defined by

$$\beta_\Gamma = |x^2 - (2 - \mu^2)x + 1|,$$

where μ is the spectral radius of the adjacency matrix of Γ. Note, this does not depend on the ordering of the vertices of Γ.

The following theorem was proved for (positively signed) classical Coxeter graphs Γ in [29].

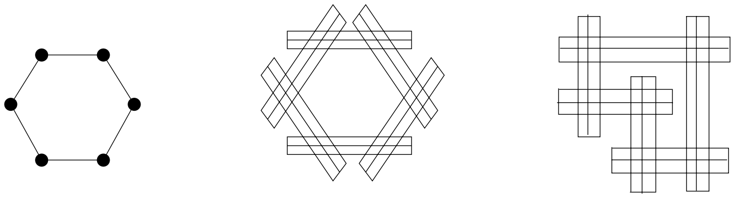

Figure 4: Two surfaces obtained from the hexagonal graph by identifying opposite short edges of the rectangles.

Theorem 2.19 *Let* Γ *be a positively signed bipartite Coxeter graph with bipartite ordering. Let* μ *be the spectral radius of the adjacency matrix of* Γ*. Then either* $|\mu^2 - 2| \leq 2$*, which implies that* $|\omega_{\Gamma,1}| = 1$*, or*

$$|\omega_{\Gamma,1}| = \beta_\Gamma$$

and hence only depends on the combinatorics of Γ*. Furthermore, for any arbitrary (positively signed) Coxeter graph* Γ*, with arbitrary ordering on the vertices,*

$$|\omega_{\Gamma,1}| \geq \beta_\Gamma.$$

In [38], Thurston gave an example of pseudo-Anosov mapping classes constructed using classical bipartite Coxeter graphs. These are mixed-sign Coxeter mapping classes associated to a bipartite Coxeter graph, with bipartite order. He proved the following.

Theorem 2.20 *If* Γ *is a classical bipartite Coxeter graph with bipartite order, then the widths and lengths of the rectangles in the construction of* S_Γ *can be chosen so that* $\phi_{\Gamma,\mathfrak{s}}$ *has constant derivative. If* ϕ_Γ *is pseudo-Anosov, then*

$$\lambda_{geo}(\phi_{\Gamma,\mathfrak{s}}) = \lambda_{hom}(\phi_{\Gamma,\mathfrak{s}}) = \beta_\Gamma.$$

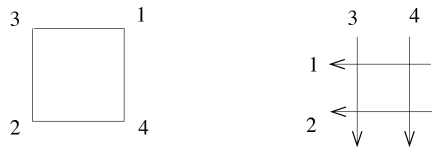

Figure 5: Dual configuration associated to a 4 cycle with bipartite ordering

Example 2.21 Consider the hexagonal graph shown Γ_6 in Figure 4. Since each vertex has order two, there is only one fatgraph structure on Γ_6. For the middle diagram, there is no way to orient the core curves on the rectangles in a way that is orientation compatible with any ordering on Γ_6. The orientation on one curve determines the orientations on its adjacent ones. Thus, a $2n$-gon has an orientation compatible diagram of this form if and only if n is even. The right diagram is compatible with the bipartite ordering. In this example, the middle surface has genus 2 and 4 boundary components, while the right hand surface has genus 3 and 2 boundary components.

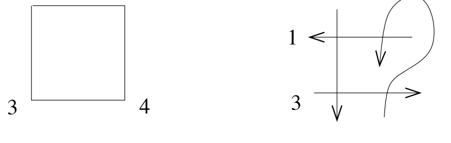

Figure 6: Dual configuration associated to a 4 cycle with cyclic ordering

Example 2.22 It also may not be possible to make the surface from a globally planar configuration of straight paths, as one can in the bipartite case. Consider for example the cyclic graph with 4

genus	mixed-sign Coxeter graph
2	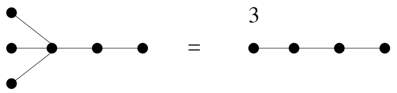
3	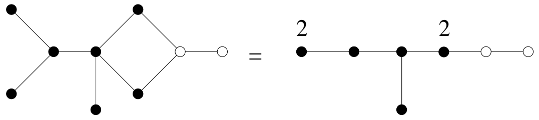
4	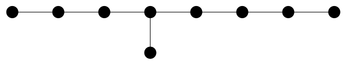
5	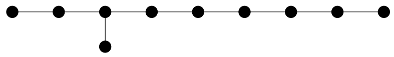

Table 1: Graphs corresponding to minimum dilatation orientable examples for $g = 2, 3, 4, 5$

vertices. The bipartite ordering gives rise to a planar configuration (see Figure 5), while for the cyclic ordering, one can verify that there is no configuration of straight line paths that realize the graph (see Figure 6). This example also illustrates that while the graph determines the Euler characteristic of the surface (with boundary), but ordering of the vertices can affect the genus. In the bipartite case, the surface has $(g, n) = (1, 4)$, while in the cyclic case the surface has $(g, n) = (2, 2)$.

2.6 Minimum dilatation orientable examples.

Table 1 displays mixed-sign Coxeter graphs that give rise to the minimum dilatation orientable mapping classes of genus 2 through 5 found by Lanneau and Thiffeault [24]. For genus 2 and 3, the equivalent integer labeled graphs are also given (see Remark 2.12). We use the convention that a filled in vertex is given the sign label '+1' while the unfilled vertex is given the sign label '-1'.

Let δ_g^+ be the minimum dilatation for an orientable pseudo-Anosov mapping class on a closed surface. The minimum orientable examples for genus $g = 2, 4, 5$ can be realized as the closures of classical Coxeter mapping classes associated to bipartite graphs constructed in [38] [25]. For genus 4 and genus 5, the graphs are the classical hyperbolic extensions of the E_7 and E_8 graphs, and in the genus 5 example, the dilatation is equal to Lehmer's number. The hyperbolic extension of E_6 is given in Figure 7. It's corresponding mapping class is defined on a surface of genus 4, but it has the same dilatation as the genus 3 example given in Table 1.

The sequence δ_g^+ converges to 1. Moreover, we have

$$\log(\delta_g^+) \asymp \frac{1}{g}$$

(see [15]). Thus, classical Coxeter mapping classes cannot realize small dilatation orientable mapping classes for high genus.

Remark 2.23 One can also study dilatations of pseudo-Anosov mapping classes (S, ϕ) in terms of the topological Euler characteristic $\chi(S)$. This is well-motivated by the following. Given a pseudo-Anosov mapping class (S, ϕ), let

$$L(S, \phi) = \lambda(\phi)^{|\chi(S)|}$$

be the *χ-normalized dilatation* of (S, ϕ). Let M be a hyperbolic 3-manifold, and F a fibered face (see [37]). Then F is a polyhedron of dimension equal to $b_1(M) - 1$ where $b_1(M)$ is the first Betti number of M. The rational points in the interior of F correspond to mapping classes (S, ϕ) that are monodromies of fibrations of M over the circle.

On any compact subset of the interior of a fibered face F the χ-normalized dilatation extends to a continuous convex function on F (see [12] [28]) and hence is bounded. Given a pseudo-Anosov (S, ϕ), let (S^0, ϕ^0) be the mapping class obtained by letting $S^0 = S \setminus \mathrm{Sing}(\phi)$, and $\phi^0 = \phi|_{S^0}$. Then (S^0, ϕ^0) is pseudo-Anosov, and $\lambda(\phi^0) = \lambda(\phi)$ (see, Lemma 2.17).

By a theorem of Farb, Leininger and Margalit [11], the collection of mapping classes (S, ϕ) with bounded *χ-normalized dilatation* correspond (after puncturing S at singularities) to rational points on compact subsets of a finite collection fibered faces.

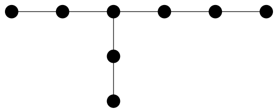

Figure 7: A positive Coxeter graph related to genus 3 example.

As an example, numerically d_3^+ equals the house of the hyperbolic extension of E_6 (see [29], Table 5, and Figure 7). Let (S_{hE_6}, ϕ_{hE_6}) be the mapping class obtained from hE_6 using the bipartite ordering. Then S_{hE_6} has genus 4 and 2 boundary components. The genus 3 example obtained from the graph Γ_3 in Table 1 has 4 boundary components. Thus, the surfaces S_{hE_6} and S_{Γ_3} have the same topological Euler characteristic.

The above discussion suggests another version of the minimum dilatation problem.

Problem 2.24 *Find the minimum dilatation of pseudo-Anosov mapping classes with no interior singularities of a given topological Euler characteristic.*

3 Twist graphs and twisted Coxeter mapping classes

In this section, we review Murasugi sums of mapping classes and define (full) twist graphs, and associated (full) twist mapping classes. Twist graphs are elementary building blocks that can be used to construct small dilatation pseudo-Anosov via Murasugi sum. In particular, we will construct sequences of mapping classes associated to iterative joins of twist graphs, and investigate conditions under which the normalized dilatations are bounded.

3.1 Murasugi sums of mapping classes.

The Murasugi sum was originally defined for fibered links in S^3 [31]. In this section we study properties of Murasugi sums for arbitrary mapping classes.

Let P_{2k} be a $2k$-sided polygon with alternate edges removed. The polygon P_{2k} is *properly embedded* in a compact surface S if the boundary components of P_{2k} are contained in the boundary of S, and the interior of P_{2k} is contained in the interior of S.

Let (S_0, ϕ_0) and (S_1, ϕ_1) be two mapping classes with proper embeddings of P_{2k}. Let S be the surface obtained by gluing S_0 and S_1 by identifying the interiors of the embedding of P_{2k} in S_0 to the interior of the embedding of P_{2k} in S_1 after rotating by $\frac{2\pi}{k}$.

Note that the intersection of the closure of $S \setminus S_i$ with S_i is contained in the boundary of S_i for $i = 0, 1$. Thus, we can extend $\phi_i : S_i \to S_i$ by the identity on $S \setminus S_i$ and let $\phi : S \to S$ be the composition $\phi = \phi_1 \circ \phi_0$. The mapping class (S, ϕ) is called the *Murasugi sum* of (S_0, ϕ_0) and (S_1, ϕ_1) relative to the embeddings of P_{2k}.

Murasugi sum and mapping tori. Let M_0 and M_1 be the mapping tori of (S_0, ϕ_0) and (S_1, ϕ_1). Identify S_i with a fiber of M_i. Let $M_i^{\Diamond}$ be the result of cutting M_i along $\iota_i(P_{2k}) \subset S_i$, creating a boundary component homeomorphic to a sphere with hemispheres identified with two copies $\iota_i(P_{2k}^+)$ and $\iota_i(P_{2k}^-)$ of P_{2k} glued together along their boundaries. Let M' be the result of gluing $M_0^{\Diamond}$ with $M_1^{\Diamond}$ along boundary spheres, so that $\iota_0(P_{2k}^+)$ is glued to $\iota_1(P_{2k}^-)$ and $\iota_0(P_{2k}^-)$ is glued to $\iota_1(P_{2k}^+)$.

Lemma 3.1 *The mapping torus M of (S, ϕ) is homeomorphic to M'.*

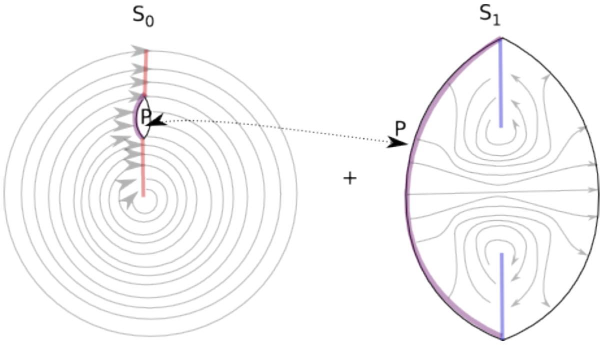

Figure 8: Murasugi sum of surface flows.

To prove Lemma 3.1 it is useful to view the mapping torus of a mapping class (S, ϕ) as a manifold with a continuous surjection

$$\mathfrak{f} : S \times [0, 1] \to M$$

such that

(i) $\mathfrak{f}$ is an embedding on $S \times [1, 0)$, and

(ii) $\mathfrak{f}(s, 1) = (\phi(s), 0)$, for $s \in S$.

An f satisfying (i) and (ii) is called a *surface flow*, with *transverse surface* S identified with $\mathfrak{f}(S \times \{0\})$, and *monodromy* (S, ϕ).

Lemma 3.2 *The map from fibrations to surface flows given by modding out the product* $S \times [0, 1]$ *by the equivalence* $(x, 1) \sim (\phi(x), 0)$ *is a bijection.*

Proof. Given a surface flow with transverse surface S and monodromy (S, ϕ), there is corresponding fibration of M over S^1 with monodromy (S, ϕ) defined by contracting the embedded surfaces $\mathfrak{f}(S \times \{t\})$. □

We relax the definition of surface flow slightly to include the following. Let $f : S \times [0, 1] \to M$ be a continuous surjective map so that (i) is replaced by

(ia) $\mathfrak{f}|_{(S \times \{t\})}$ is 1-1 for all $t \in [0, 1]$; and

(ib) $f(s, t) = f(s', t')$ only if $s = s'$ and for all $t_1 \in [t, t']$, $f(s, t_1) = f(s, t)$.

Given a flow f satisfying $(ia), (ib)$ and (ii), one can continuously deform f until it satisfies (i) and (ii), and hence f determines a unique fibration of M with fiber S. We will use this weaker version of surface flow in what follows.

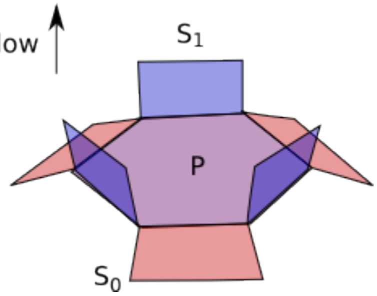

Figure 9: Local gluing of S_0 and S_1 at P with upward surface flow.

Proof of Lemma 3.1. Let $P = P_{2k}$, and let $(M_i, S_i, \mathfrak{f}_i)$ be two flows defined (up to isotopy) by (S_i, ϕ_i), for $i = 0, 1$.. Define a flow $(M, S, \mathfrak{f})$ by $\mathfrak{f} : S \times [0, 1] \to M$, where

$$f(s,t) = \begin{cases} \mathfrak{f}_0(s, 2t) & \text{if } s \in S_0,\ 0 \le t \le 1/2 \\ \mathfrak{f}_1(s, 0) & \text{if } s \in S_1 \setminus \iota_1(P),\ 0 \le t \le 1/2 \\ \mathfrak{f}_0(s, 1) & \text{if } s \in S_0 \setminus \iota_0(P),\ 1/2 \le t \le 1 \\ \mathfrak{f}_1(s, 2t-1) & \text{if } s \in S_1,\ 1/2 \le t \le 1 \end{cases}$$

The sum of the flows is illustrated in Figure 8. The monodromy ϕ is the isotopy type of the composition $f_1 \circ f_0$. Figure 9 illustrates the local gluing of S_0 and S_1. The map f defines a unique surface flow on M up to isotopy, and hence a fibration of

$$M \to S^1,$$

with monodromy equal to the Murasugi sum of $(S_0, \phi_0$ and (S_1, ϕ_1). $\square$

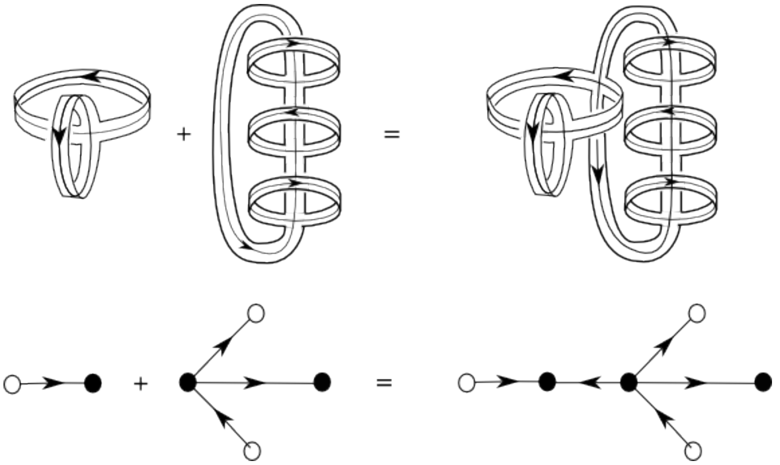

Figure 10: Join of graphs, and corresponding geometric realization.

Example 3.3 Let $\Gamma_i = (\mathcal{V}_i, \mathcal{E}_i)$, $i = 0, 1$ be two mixed-sign Coxeter graphs, and let $v_i \in \mathcal{V}_i$ be fixed vertices. Then the *join* of Γ_0 and Γ_1 at v_0 and v_1 is the graph obtained by taking the disjoint union of Γ_0 and Γ_1 and adding a new edge ϵ between v_0 and v_1. If Γ_0 and Γ_1 are ordered and have fatgraph structure at their vertices, then the *join* is determined by the choice of element $w_i \in \mathcal{V}_{v_i}$ for each $i = 1, 2$. Then v_1 is inserted into $\mathcal{V}_{v_2}$ after w_2, and similarly v_2 is inserted into $\mathcal{V}_{v_1}$ after w_1.

Assume that Γ_i are simply-laced Coxeter graphs with global orderings and local fatgraph structure, let $\mathfrak{s}_i$, $i = 0, 1$ be sign labels on $\mathcal{V}_i$, and let $(S_{\Gamma_i, \mathfrak{s}_i}, \phi_{\Gamma_i, \mathfrak{s}_i})$ be the corresponding Coxeter mapping class. Then for any choice of pairs of adjacent edges at v_0 and v_1, we have a new mixed-sign Coxeter graph with global and local fatgraph structure $(\Gamma, \mathfrak{s})$, and the Coxeter mapping class $(S_{\Gamma,\mathfrak{s}}, \phi_{\Gamma,\mathfrak{s}})$ is obtained from $(S_{\Gamma_i}, \mathfrak{s}_i)$ by Murasugi sum along square a P_4.

Figure 10 shows an example. Although the graphs are drawn with sign-labelings, the geometric realizations only depend on the underlying ordered fatgraphs.

3.2 Full twist braids and their monodromy.

In this section, we will define twist maps and twist graphs, and use them as building blocks for constructing sequences of mixed-sign Coxeter mapping classes. The twist maps $(\Sigma_m^{(k)}, R_m^{(k)})$, $m \geq 2$, $k \geq 1$, have the following properties

1. $(\Sigma_m^{(k)}, R_m^{(k)})$ is the Coxeter mapping class associated to a graph with $\mathfrak{s} \equiv -1$;

2. $(R_m^{(k)})^{km}$ is a product of left Dehn twists on the boundary components of Σ_m; and
3. the mapping class $R_m^{(k)}$ preserves a flat structure on $\Sigma_m^{(k)}$ with a periodic orbit O of order km, and the mapping torus of the restrictions $(\Sigma_m^{(k)} \setminus \mathrm{O}, R_m^{(k)}|_{(\Sigma_m^{(k)} \setminus \mathrm{O})})$ are independent of k.

Let $b_m^{(k)}$ be the product of k full twist braids on m strands. Consider the link $L_m^{(k)}$ in S^3 defined by $b_m^{(k)}$ with an encircling link E. The case where $m = 5$ and $k = 1$ is illustrated in Figure 11. The complement of a tubular neigborhood $L_m \cup E$ in S^3 can be identified with the product of a circle with the surface $S_{0,m+1}$ with genus 0 and $m + 1$ boundary components, and thus is independent of k.

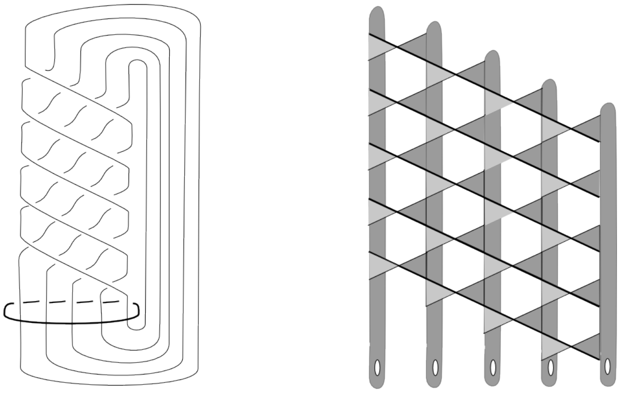

Figure 11: Closure of a full twist braid on 5 strands, and a fiber surface.

Consider the fibration of $S^3 \setminus L_m^{(k)} \cup E$ with fiber equal to the surface $\Sigma_m^{(k)}$ drawn on the right in Figure 11. The monodromy is periodic of order km (modulo the action near the boundary), and can be seen explicitly as follows.

The surface $\Sigma_m^{(k)}$ is a union of m *main* disks (drawn vertically in Figure 11) and km *attaching* disks (drawn horirzontally). We can think of the darkly shaded regions as being the positively oriented side of $\Sigma_m^{(k)}$, and the lightly shaded region as being on the negatively oriented side. Number the main disks from right to left $d_1, \ldots, d_m$ and the attaching disks $a_1, \ldots, a_{km}$ from top to bottom. Then the monodromy acts by cyclically permuting the main disks

$$d_1 \to d_2 \to \cdots \to d_m \to d_1$$

while rotating them by $\frac{2\pi}{km}$, and the attaching disks

$$a_1 \to a_2 \to \cdots \to a_{km} \to a_1,$$

while rotating them by $\frac{2\pi}{m}$. The mapping class $R_m^{(k)}$ has the property that $(R_m^{(k)})^m$ rotates the interiors of each of the disks by 360 degrees in the counter-clockwise direction. In other words, it is isotopic to the product of left Dehn twists along boundary parallel curves. Thus we have the following.

Lemma 3.4 *The twist mapping class R_m has the property that*

$$(R_m^{(k)})^{km} = (\partial_1 \circ \partial_2 \circ \cdots \partial_m)^{-1}$$

where ∂_i is a positive Dehn twist around the ith boundary component of Σ_m. (Here, the ordering does not matter, since the Dehn twists on the right hand side of the equation commute.)

We now show that the mapping classes $(\Sigma_m^{(k)}, R_m^{(k)})$ are the partial closures of mixed-sign Coxeter mapping classes.

Consider the graph T_m with $(m-1) \times (m-1)$ vertices shown in the right diagram of Figure 12. Order the vertices on the graph T_m in any way that is compatible with the arrows, and label all vertices -1. Denote the signed graph by $(T_m, -1)$. The left diagram shows a picture of Σ_m and the middle diagram gives a blow up of the oriented simple closed curves corresponding to the vertices of T_m verifying that $(T_m, -1)$ has the correct incidences.

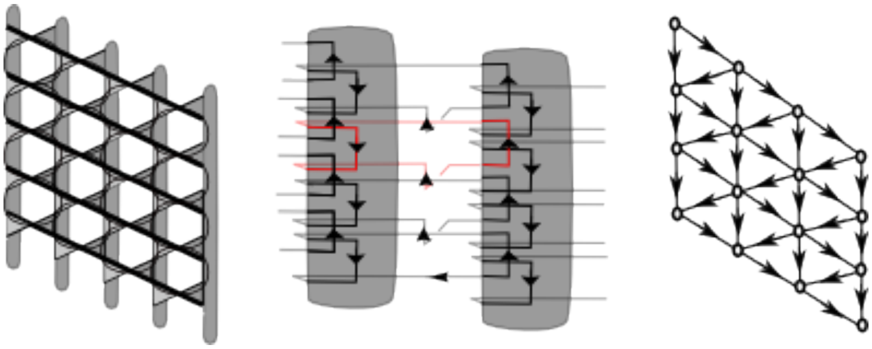

Figure 12: Mixed-sign Coxeter graph $(T_m, -1)$ realized by R_m, for $m = 5$.

Lemma 3.5 *The twist mapping class (Σ_m, R_m) is the Coxeter mapping class for the graph $(T_m, -1)$ closed over all but m of its boundary components.*

Proof. Let (Y_m, f_m) be the mixed sign Coxeter mapping class associated to $(T_m, -1)$.

By inspecting the intersections of the loops drawn on the left and middle diagrams of Figure 12, one sees that their intersection graph is equal to T_m. Thus, Y_m embeds in S_m and $S_m \setminus Y_m$ is a union of disks in the interior of S_m.

Observe that the embedding of S_m in S^3 can be inductively defined as the union of negatively twisted Hopf bands: one starts with a single negatively twisted Hopf band, corresponding to the top most vertex of T_m; then the surface obtained at the nth stage of the inductive process equals the union of the surface obtained at the $(n-1)$st stage by attaching a Hopf plumbing along an embedded square. By the theory of Murasugi sums reviewed in Section 3.1, it follows that the extension of f_m to Σ_m equals R_m, and thus the partial closure of (Y_m, f_m) is (Σ_m, R_m) as required.
□

Remark 3.6 A Coxeter system is *spherical* if its associated bilinear form is positive or negative definite, and it is *affine* if its bilinear form is positive or negative semi-definite. In the classical case, where $\mathfrak{s} \equiv 1$, the Coxeter system is spherical or affine if and only if a Coxeter element has spectral radius equal to 1. The graphs $(T_m, -1)$ are examples of mixed-sign Coxeter systems whose Coxeter element has spectral radius one, but is not spherical or affine (for example, the Coxeter group contains hyperbolic elements).

Problem 3.7 *Classify the mixed-sign Coxeter systems.*

Flat structure. Give each $d_1, \ldots, d_m$ and $a_1, \ldots, a_m$ the flat structure of regular m-gons. Then R_m preserves the induced singular flat structure on Σ_m. More precisely, the m-gons $d_1, \ldots, d_m$, and $a_1, \ldots, a_m$ are each permuted cyclically, preserving centers and rotating the m-gons by an angle of $\frac{\pi}{m}$.

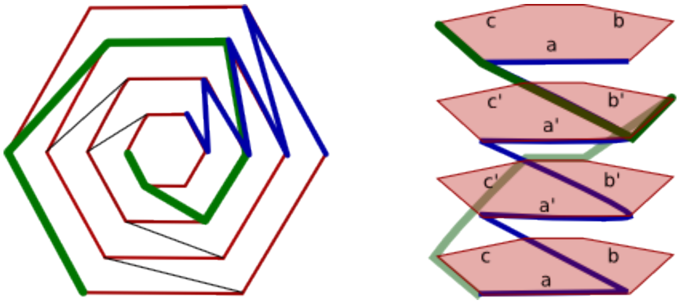

Figure 13: The main disks $d_1, \ldots, d_m, d_{m+1}$, where d_{m+1} is identified with d_1 $(m = 3)$.

Figure 13 shows two views of Σ_m for $m = 3$. The left-most figure shows a view of the surface with boundary, where one of the three boundary curves is drawn spiraling inward. The 3-gons d_1, d_2, d_3 are drawn as hexagons (the innermost hexagon is identified with the outermost hexagon), and the boundary of one of the hexagons a_i is drawn as a zigzag. The right-hand figure gives a side view, where the top hexagon corresponds to the inner hexagon in the left hand diagram. Again the bottom hexagon is identified with the top hexagon. The map R_m takes each d_i and a_i and rotates by an angle of $\frac{\pi}{3}$ in the counter-clockwise direction.

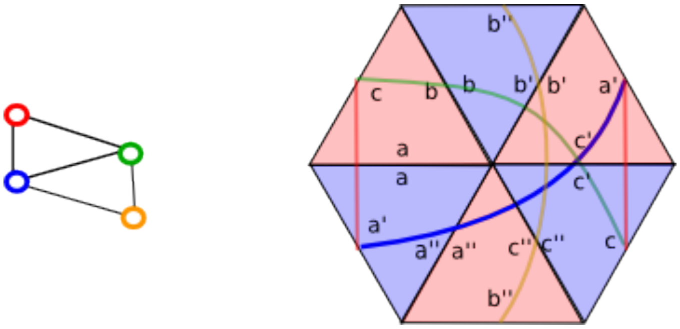

Figure 14: Two views of the twist surface (homeomorphic to a torus) for $m = 3$.

If we shrink the boundary of Σ_m to a point, then the resulting surface can be given a flat structure as the union of $2m$ regular m-gons of equal size. To visualize the flat structure on the closure $\overline{\Sigma}_m$, one contracts the spiraling boundary curves. For example, $\overline{\Sigma}_3$ is a torus, and R_3 preserves its structure as a union of six equilateral triangles. In Figure 14 the surface $\overline{\Sigma}_3$ and its flat structure

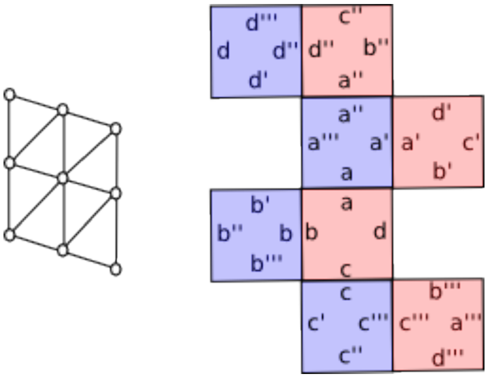

Figure 15: The twist surface for $m = 4$.

are shown. Sides labeled with the same symbol are identified. One can see that $\overline{\Sigma}_3$ is a translation surface.

The map R_4 preserves the structure of $\overline{\Sigma}_4$ as the union of 8 squares (Figure 15). Again, we see that $\overline{\Sigma}_4$ is a translation surface. While the flat structure on $\overline{\Sigma}_3$ has no singularities, the flat structure on $\overline{\Sigma}_4$ has 4 singularities of degree 2.

3.3 Iterated Murasugi sum with twist maps

Let $(\Gamma, \mathfrak{s})$ be a mixed-sign Coxeter mapping class containing $(A_m, -1)$ as a subgraph, where A_m is the standard spherical Coxeter graph. We will define an extended m-twist graph $(\widetilde{T}_m, -1)$ with a distinguished $(A_m, -1)$-subgraph, and define a sequence of graphs $(\Gamma_k, \mathfrak{s}_k)$ obtained by iteratively joining the extended m-twist graphs.

By an extended m-twist graph, we mean the graph with $m(m-1)$ vertices shown in Figure 16 center. The right graph in Figure 16 is the k times iterated m-twist graph $(T_m^k, -1)$ for $k = 3$.

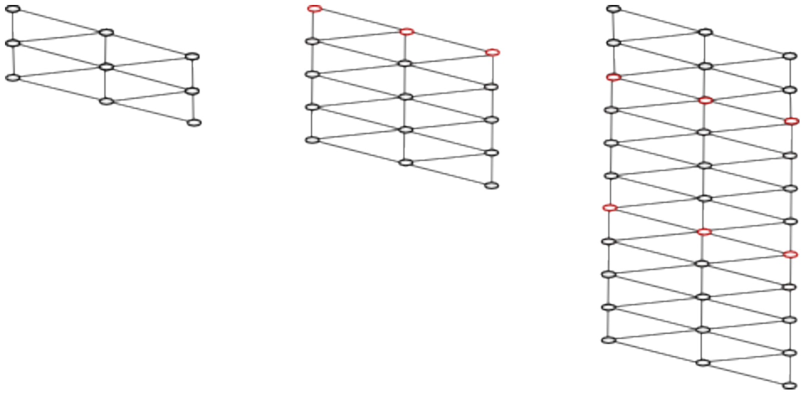

Figure 16: The twist graph (left) extended twist graph (center) and iterated twist graph (right) for $m = 4$ and $k = 3$.

Let $(\Sigma_m^{(k)}, R_m^{(k)})$ be the Coxeter mapping classes associated to $(T_m^k, -1)$ after closing over all but m

boundary components as in Figure twistgraphsurface-fig.

Lemma 3.8 *For $k \geq 1$, the mapping torus for $(\Sigma_m^{(k)}, R_m^{(k)})$ is homeomorphic to the link complement of L in S^3, where L is the closure of a full twist braid and its encircling link.*

The link L is drawn in Figure 11. Now consider a general mixed-sign Coxeter graph $(\Gamma, \mathfrak{s})$ containing an $(A_m, -1)$ subgraph. Let (S_k, ϕ_k) be the mapping class obtained by joining $(\Gamma, \mathfrak{s})$ to the extended $(T_m^{(k)}, -1)$ along $(A_m, -1)$.

Lemma 3.9 *The mapping tori for (S_k^0, ϕ_k^0) are all contained in a single homeomorphism class M of 3-manifolds for all $k \geq 1$, and the mapping tori M_k for (S_k, ϕ_k) are Dehn fillings of M along the tubular neighborhood N of the suspension of O, with slope $[1 : k]$ with respect to some fixed choice of generators of $\pi_1(N)$.*

Proof. The mapping torus M_k is obtained by taking the mapping torus for (S, ϕ), removing a ball neighborhood of P, and inserting the mapping torus of $(\Sigma_m^{(k)}, R_m^{(k)})$ as in Figure 8. Figure 13. After deleting N, the mapping tori of (Σ_m, R_m) are all identical. This is because, each full twist corresponds to Dehn filling on N by a $[1 : k]$ -slope. Since N is disjoint from the attaching locus, the homeomorphism type of M_k^0 is independent of k. □

Remark 3.10 The proof above also applies to the Murasugi sum of an arbitrary mapping class (S, ϕ) with a properly embedded P_{2m} with the mixed-sign Coxeter mapping classes associated to $(T_m^{(k)}, -1)$.

Attaching tails, and iterated Hopf plumbing.

Consider the special case when $m = 1$. Then the corresponding Coxeter graph is $(A_k, -1)$, where A_k is the classical spherical Coxeter system. In this case, since A_k is a tree, and hence bipartite (see Section 2.5) the signs on the vertices (in this case "-1") can be replaced by 1, and we can take $T_2^{(k)}$ to be the classical A_k diagram.

Let (S, ϕ) is any mapping class with an attaching square, and (S_k, ϕ_k) is the sequence of mapping classes obtained by attaching $(\Sigma_1^{(k)}, R_1^{(k)})$. We call (S_k, ϕ_k) the sequence of mapping classes obtained from (S, ϕ) by *attaching a tail.*

A *Salem-Boyd* sequence of polynomials is a sequence of the form

$$P_k(x) = x^k Q(x) + Q^*(x)$$

where $Q(x)$ is a monic integer polynomial, and $Q^*(x) = x^{\deg(Q)} Q(1/x)$ is the *reciprocal* of $Q(x)$. These sequences were used in [36] and [6] to study properties of Salem numbers. The house $|P_k|$ of P_k has the following properties (see, [13] Theorem 12).

Theorem 3.11 *If $P_k(x) = x^k Q(x) + Q^*(x)$ is a Salem-Boyd sequence, then*

(i) the number of roots of P_k outside the unit circle is monotone increasing, and eventually constant, and

(ii) $\lim_{k\to\infty} |P_k| = |Q_k|$.

Mapping classes (S_k, ϕ_k) corresponding to graphs with tails are studied in [13] in the case when the graph is dual to a chord system on a disk. In this case, it is shown that the mapping classes are the monodromy of a sequence of links L_k in S^3, obtained from a single fibered link L_0 by twisting a suitable pair of strands. Furthermore, the Alexander polynomial, or characteristic polynomial of the action of ϕ_k on first homology, is a Salem-Boyd sequence. The proof (see [13], Theorem 9) relies only on the form of $(\phi_k)_*$ given in Theorem 2.8 and Theorem 2.13.

Theorem 3.12 ([13], Theorem 9) *The Alexander polynomial Δ_k corresponding to (S_k, ϕ_k) is a Salem-Boyd sequence, and hence the homological dilatations $\lambda_{hom}(\phi_k)$ form a convergent sequence.*

Corollary 3.13 *Let (S_k, ϕ_k) be obtained by attaching a single tail to a mapping class (S, ϕ). Then either*

(i) $\lambda_{hom}(\phi_k) = 0$ for all k, or

(ii) $|\Delta_k|$ converges to a real number greater than one.

Proof. This follows from Theorem 3.12 and Theorem 3.11. □

Corollary 3.14 *Let $(\Gamma, \mathfrak{s})$ be a connected mixed-sign Coxeter graph, $v \in \mathcal{V}$ a distinguished vertex, and $(\Gamma_k, \mathfrak{s}_k)$ the join of $\Gamma, \mathfrak{s}$ with $(A_k, \mathfrak{s}(v))$. Let (S_k, ϕ_k) be any Coxeter mapping class associated to $(\Gamma_k, \mathfrak{s}_k)$. Then either*

(i) ϕ_k is periodic,

(ii) ϕ_k is pseudo-Anosov, but $\lambda_{hom}(\phi_k) = 0$ for all k, or

(iii) for large k, ϕ_k is pseudo-Anosov, and there is a constant C such that

$$\lambda(\phi_k) \geq C > 1.$$

Proof. Since Γ is connected, each ϕ_k is either periodic, or ϕ_k is pseudo-Anosov. If $|\Delta_k| > 1$ for some k, then, by Corollary 3.13, $\lambda_{\text{hom}}(\phi_k) = |\Delta_k|$ is greater than one for k large enough. In this case, by Theorem 2.14, ϕ_k is pseudo-Anosov, and, for any $\epsilon > 0$, $\lambda(\phi_k) \geq \ell - \epsilon$, where $\ell = \lim_{k\to\infty} |\Delta_k|$. □

Example 3.15 Let $(\Gamma_{m,n}, \mathfrak{s})$ be the graph in Figure 17. Since $T_1^{(k)}$ is a bipartite graph, and hence (by Theorem 2.18) it is interchangeable with the standard A_n-Coxeter graph with all signs positive. Thus, we can think of this graph as being obtained from the connected two vertex graph with opposite sign labels on the vertices by joining m and n iterated twist graphs of width $r = 1$. Since the graph is bipartite, the ordering of the vertices does not change value of $|\omega_{\Gamma_{m,n},\mathfrak{s}}|$. Let $(S_{m,n}, \phi_{m,n})$ be the mapping class associated to $(\Gamma_{m,n}, \mathfrak{s})$. The surface $S_{m,n}$ has genus

$$g_{m,n} = \left[\frac{m+n}{2}\right],$$

and one or two boundary components, according to whether $m+n$ is even or odd. Here $[a]$ denotes the greatest integer less than or equal to a real number a. In particular, $g_{m,m} = m$.

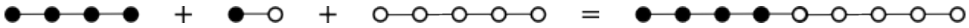

Figure 17: mixed-sign Coxeter graph $(\Gamma_{4,5}, \mathfrak{s})$ obtained by joining twist graphs of width 1.

The mapping classes $(S_{m,n}, \phi_{m,n})$ have also been studied in a different form by P. Brinkmann [7] and [15] (cf. [39]), yielding the following.

Theorem 3.16 (Brinkmann [7], Hironaka-Kin [15], Tsai [39]) *For all m, n, $(S_{m,n}, \phi_{m,n})$ is pseudo-Anosov, and for fixed $m+n$, the dilatation is minimized when $m = n$. Furthermore,*

$$\log(\lambda(\phi_{g,g})) \asymp \frac{\log(g)}{g}.$$

The following question is open.

Question 3.17 *Is there a mixed-sign Coxeter graph $(\Gamma, \mathfrak{s})$ with vertices $v_1, \dots, v_m$ (possibly counted with multiplicity) so that the mapping classes $(S_{\overline{k}}, \phi_{\overline{k}})$ associated to the joins of $(\Gamma, \mathfrak{s})$ with iterated k_i- twists of width 1 at each of the v_i, $\overline{k} = (k_1, \dots, k_m)$, has the asymptotic behavior*

$$\log(\lambda(\phi_{\overline{k}})) \asymp \frac{1}{g_{\overline{k}}}, \tag{4}$$

where and $g_{\overline{k}}$ is the genus of $S_{\overline{k}}$?

3.4 Asymptotically small dilatation Coxeter mapping classes.

In this section, we prove Theorem 1.2 by showing the existence of a sequence of mixed-sign Coxeter mapping classes (S_k, ϕ_k) whose closures $(\overline{S}_k, \overline{\phi}_k)$ have the following properties:

(i) $\overline{\phi}_k$ is pseudo-Anosov,

(ii) the associated stable and unstable foliations are orientable,

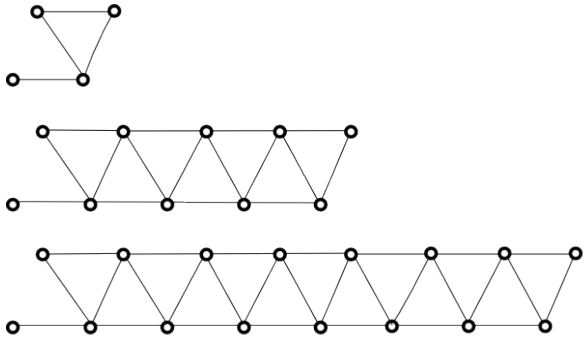

Figure 18: A negatively signed Coxeter fatgraph for $k = 1$, $k = 2$ and $k = 3$.

(iii) $\overline{S}_k$ has monotone increasing genus g_k,

(iv) $\lambda(\overline{\phi}_k)$ approaches 1, and furthermore

$$\lim_{k\to\infty} \lambda(\overline{\phi}_k^{g_k}) = \frac{3+\sqrt{5}}{2},$$

the smallest known accumulation point of genus-normalized dilatations.

The mapping classes (S_k, ϕ_k) are obtained from the mixed-sign Coxeter mapping classes corresponding to the negatively signed graphs Γ_k drawn in Figure 18 by closing over all but 3 boundary components. The graphs are given their fatgraph structures as planar graphs.

To show that the mapping classes (S_k, ϕ_k) satisfy the conditions (i)-(iv), we relate them to the monodromy of the links drawn in 19. The figure shows pairs of equivalent link diagrams for the mapping tori of (S_k, ϕ_k), $k = 1, 2$. In the left versions the shaded region shows the contribution of the copies of (Σ_3, R_3). The links beside them on the right shows an equivalent positive braid version of the links. The graphs Γ_k give rise to the Seifert surfaces corresponding to the latter planar projection of the links after closing over suitable boundary components.

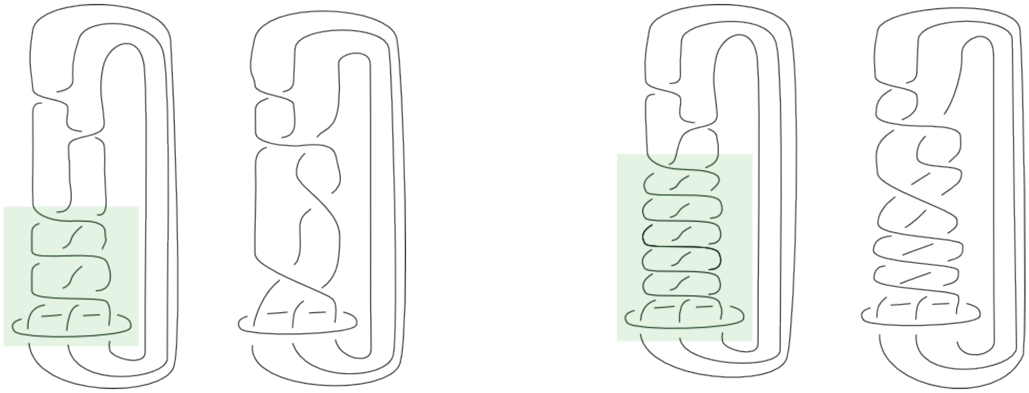

Figure 19: Link diagram for S_k, ϕ_k, for $k = 1, 2$.

Lemma 3.18 *The mapping classes (S_k, ϕ_k) corresponding to $(\Gamma_k, -1)$ satisfy (i)-(iv).*

By Lemma 3.9, the mapping tori for (S_k^0, ϕ_k^0) belong to a single homeomorphism class, in this case, it is the complement M of the 6_2^2-link L in S^3 (see, the knot table in [33]). The link is shown in Figure 20.

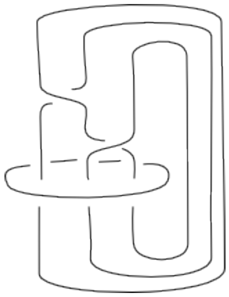

Figure 20: The 6_2^2-link.

The mapping class, written as $\phi_0 = \sigma_1\sigma_2^{-1}$ in terms of the standard braid generators, is known as the simplest hyperbolic braid monodromy, The fibered face defined by the braid monodromy ϕ_0 shown in the link diagram in Figure 20 was studied in [14]. The link L has two components, K_1 corresponds to the strands of the braid, and K_2 is the encircling link. Let $t \in H_1(M, \mathbb{Z})$ be the meridian loop around K_1 and let $u \in H_1(M; \mathbb{Z})$ be the meridian loop around K_2. Let ξ be the dual to t and ψ the dual to u in $H^1(M; \mathbb{Z})$. Then ψ is the fibration of M corresponding to the braid monodromy ϕ_0. Given a fibration $\alpha : M \to S^1$, there is a corresponding element of $H^1(M; \mathbb{Z})$ defined by the induced map $\alpha_* : H_1(M; \mathbb{Z}) \to \mathbb{Z}$, and hence we can write

$$\alpha_* = a\psi + b\xi.$$

The integers a and b are determined by the condition that α_* restricted to $H_1(S_\alpha; \mathbb{Z})$ is trivial, where S_α is any fiber of α.

For each k, we will show that (S_k, ϕ_k) is the monodromy of $6k\psi + \xi$. The link diagrams for (S_k, ϕ_k) can be obtained from that of the 6_2^2-link shown in Figure 20, by removing a tubular neighborhood of K_2, and refilling with meridian μ_2', where

$$\mu_2' = \mu_2 - k\ell_2.$$

Under the induced homomorphisms $\psi_*, \xi_* : H_1(M; \mathbb{Z}) \to H_1(S^1; \mathbb{Z}) = \mathbb{Z}$,, we have $\psi_*(\mu_2') = 1$, and $\xi_*(\mu_2') = -3k$. Thus, (S_k, ϕ_k) is the monodromy of the fibration defined by $\psi_k = 3k\psi + \xi$.

The homological and geometric dilatations of (S_k, ϕ_k) can be computed from the Teichmüller and Alexander polynomials of M. Since 6_2^2 is a symmetric braid (that is, if one can move the link isotopically to get the same link diagram with K_1 and K_2 switched) it follows that the fibered face for ψ and invariants like the Teichmüller polynomial are the same as those of the fibered face for ξ (after switching variables). For the 6_2^2-link complement, the Thurson norm is defined by

$$||(a, b)|| = \max\{|2a|, |2b|\},$$

so for $k > 1$, ψ_k lies in the fibered face containing ξ, and the rays through ψ_k in $H^1(M; \mathbb{R})$ converge to the ray through ξ. Using the computations in [28] and [14], we have the following.

Corollary 3.19 *The mapping classes (S_k, ϕ_k) have genus $3k - 1$.*

Proposition 3.20 *The homological and geometric dilatations of (S_k, ϕ_k) are given by*

$$\lambda_{geo}(\phi_k) = \lambda(\phi_k) = |LT_{1,3k}| = |x^{6k} - x^{2k+1} - x^{3k} - x^{3k-1} + 1|,$$

and

$$\lambda_{hom}(\phi_k) = |x^{6k} - x^{3k+1} + x^{3k} - x^{3k-1} + 1|.$$

Corollary 3.21 *When k is even, then (S_k, ϕ_k) is orientable, and attains Lanneau and Thiffeault's conjectural minimum dilatation for orientable pseudo-Anosov mapping classes on closed surfaces of even genus.*

Corollary 3.22 *The mapping class (S_2, ϕ_2) is a minimum dilatation orientable mapping class for genus $g = 5$..*

The following was proved (in stronger form) in [14] using fibered face theory.

Lemma 3.23

$$\lim_{k\to\infty} \lambda(\phi_k)^{3k} = \frac{3+\sqrt{5}}{2}.$$

This completes the proof of Theorem 1.2.

References

[1] J. Aaber and N. Dunfield. Closed surface bundles of least volume. *Algebr. Geom. Topology*, 10:2315–2342, 2010.

[2] N. A'Campo. Sur les valeurs propres de la transformation de Coxeter. *Invent. Math.*, 33(1):61–67, 1976.

[3] J. Armstrong. Principal elements of mixed-sign coxeter systems. *Florida State Univeristy, PhD. Thesis*, 2012.

[4] J. Birman. *Braids, links, and mapping class groups.* Number 82 in Annals of Math. Studies. Princeton University Press, Princeton, NJ, 1974.

[5] N. Bourbaki. *Groupes et algèbres de Lie.* Hermann, Paris, 1968.

[6] D.W. Boyd. Small Salem numbers. *Duke Math. J.*, 44(2):315–328, 1977.

[7] P. Brinkmann. A note on pseudo-Anosov maps with small growth rate. *Experimental Math.*, 13(1):49–53, 2004.

[8] J. Cho and J. Ham. The minimal dilatation of a genus two surface. *Experiment. Math.*, 17:257–267, 2008.

[9] M. Dehn. Die gruppe der abbildungsklassen. *Acta Math.*, 69, 1938.

[10] I. Dolgachev. Reflection groups in algebraic geometry. *Bull. of the A.M.S.*, 45(1):1–60.

[11] B. Farb, C. Leininger, and D. Margalit. Small dilatation pseudo-anosovs and 3-manifolds. *preprint*, 2009.

[12] D. Fried. Flow equivalence, hyperbolic systems and a new zeta function for flows. *Comment. Math. Helvetici*, 57:237–259, 1982.

[13] E. Hironaka. Chord diagrams and Coxeter links. *J. London Math. Soc.*, 69(2):243–257, 2004.

[14] E. Hironaka. Small dilatation pseudo-Anosov mapping classes coming from the simplest hyperbolic braid. *Algebr. Geom. Topol.*, 10:2041–2060, 2010.

[15] E. Hironaka and E. Kin. A family of pseudo-Anosov braids with small dilatation. *Algebr. Geom. Topol.*, 6:699–738, 2006.

[16] F. Hirzebruch. über singularitäten komplexer flächen. *Rend. Math. Appl.*, pages 213–232, 1966.

[17] F. Hirzebruch. Involutionen auf mannigfaltigkeiten. In *Proceedings of the Conference on Transformation groups, New Orleans 1967*, pages 148–166. Springer, 1968.

[18] R. Howlett. Coxeter groups and M-matrices. *Bull. London Math. Soc.*, 14(2):137–141, 1982.

[19] J. Humphreys. *Reflection groups and Coxeter groups.* Cambridge University Press, Cambridge, 1990.

[20] S. Humphries. *Generators of the mapping class group*, volume 722, pages 44–47. Springer, 1979.

[21] E. Kin and M. Takasawa. Pseudo-anosovs on closed surfaces having small entropy and the whitehead sister link exterior. *J. Math. Soc. Japan*, (to appear), 2011.

[22] C. Labruère. Generalized braid groups and mapping class groups. *J. Knot Theory Ramifications*, 6(5):715–726, 1997.

[23] C. Labruère and L. Paris. Presentations for the punctured mapping class groups in terms of Artin groups. *Algebr. Geom. Topol.*, 1:73–114, 2001.

[24] E. Lanneau and J-L Thiffeault. On the minimum dilatation of pseudo-Anosov homeomorphisms on surfaces of small genus. *Ann. de l'Inst. Four.*, 61(1):164–182, 2011.

[25] C. Leininger. On groups generated by two positive multi-twists: Teichmuller curves and Lehmer's number. *Geometry & Topology*, 88:1301–1359, 2004.

[26] W.B.R. Lickorish. *An Introduction to Knot Theory.* Springer, 1997.

[27] M. Matsumoto. A simple presentation of mapping class groups in terms of Artin groups. *Sugaku Expositions*, 15(2):223–236, 2002.

[28] C. McMullen. Polynomial invariants for fibered 3-manifolds and Teichmüller geodesics for foliations. *Ann. Sci. École Norm. Sup.*, 33:519–560, 2000.

[29] C. McMullen. Coxeter groups, Salem numbers and the Hilbert metric. *Publ. Math. Inst. Hautes Études Sci.*, 95:151–183, 2002.

[30] C. McMullen. Prym varieties and Teichmüller curves. *Duke Math J.*, 133(3):569–590, 2006.

[31] K. Murasugi. On the genus of the alternating knot. i,ii. *J. Math.Soc. Japan*, 104:94–105,235–248, 1958.

[32] R. Penner. Bounds on least dilatations. *Proceedings of the A.M.S.*, 113(2):443–450, 1991.

[33] D. Rolfsen. *Knots and Links.* Publish or Perish, Inc, Berkeley, 1976.

[34] E. Rykken. Expanding factors for pseudo-Anosov homeomorphisms. *Michigan Math. J.*, 46(2):281–296, 1999.

[35] K. Saito. Around the theory of the generalized weight system: relations with singularity theory the generalized weyl group and its invariant theory, etc. *Amer. Math. Soc. Transl. (2)*, 183:101–143, 1998.

[36] R. Salem. A remarkable class of algebraic integers. proof of a conjecture of vijayaraghavan. *Duke Math. J.*, 11:103–108, 1944.

[37] W. Thurston. A norm for the homology of 3-manifolds. *Mem. Amer. Math. Soc.*, 339:99–130, 1986.

[38] W. Thurston. On the geometry and dynamics of diffeomorphisms of surfaces. *Bull. Amer. Math. Soc. (N.S.)*, 19(2):417–431, 1988.

[39] C. Tsai. The aymptotic behavior of least pseudo-Anosov dilatations. *Geometry and Topology*, 13:2253–2278, 2009.

[40] O.V. Lyashko V. I. Arnold, V.V. Goryunov and V.A.Vasil'ev. *Singularity Theory I.* Springer-Verlag, Berlin, 1991.

[41] B. Wajnryb. A simple presentation for the mapping class group of an orientable surface. *Israel J. Math.*, 45:157–174, 1983.